minerals

MDPI

Article

Eliopoulosite, V_7S_8, A New Sulfide from the Podiform Chromitite of the Othrys Ophiolite, Greece

Luca Bindi [1,*], Federica Zaccarini [2], Paola Bonazzi [1], Tassos Grammatikopoulos [3], Basilios Tsikouras [4], Chris Stanley [5] and Giorgio Garuti [2]

1 Dipartimento di Scienze della Terra, Università degli Studi di Firenze, I-50121 Florence, Italy; paola.bonazzi@unifi.it
2 Department of Applied Geological Sciences and Geophysics, University of Leoben, A-8700 Leoben, Austria; federica.zaccarini@unileoben.ac.at (F.Z.); giorgio.garuti1945@gmail.com (G.G.)
3 SGS Canada Inc., 185 Concession Street, PO 4300, Lakefield, ON K0L 2H0, Canada; Tassos.Grammatikopoulos@sgs.com
4 Faculty of Science, Physical and Geological Sciences, Universiti Brunei Darussalam, BE 1410 Gadong, Brunei Darussalam; basilios.tsikouras@ubd.edu.bn
5 Department of Earth Sciences, Natural History Museum, London SW7 5BD, UK; c.stanley@nhm.ac.uk
* Correspondence: luca.bindi@unifi.it; Tel.: +39-055-275-7532

Received: 22 February 2020; Accepted: 6 March 2020; Published: 8 March 2020

Abstract: The new mineral species, eliopoulosite, V_7S_8, was discovered in the abandoned chromium mine of Agios Stefanos of the Othrys ophiolite, located in central Greece. The investigated samples consist of massive chromitite hosted in a strongly altered mantle tectonite, and are associated with nickelphosphide, awaruite, tsikourasite, and grammatikopoulosite. Eliopoulosite is brittle and has a metallic luster. In plane-reflected polarized light, it is grayish-brown and shows no internal reflections, bireflectance, and pleochroism. It is weakly anisotropic, with colors varying from light to dark greenish. Reflectance values of mineral in air (R_o, $R_{e'}$ in %) are: 34.8–35.7 at 470 nm, 38–39 at 546 nm, 40–41.3 at 589 nm, and 42.5–44.2 at 650 nm. Electron-microprobe analyses yielded a mean composition (wt.%) of: S 41.78, V 54.11, Ni 1.71, Fe 1.1, Co 0.67, and Mo 0.66, totali 100.03. On the basis of Σ_{atoms} = 15 apfu and taking into account the structural data, the empirical formula of eliopoulosite is $(V_{6.55}Ni_{0.19}Fe_{0.12}Co_{0.07}Mo_{0.04})_{\Sigma=6.97}S_{8.03}$. The simplified formula is $(V, Ni, Fe)_7S_8$ and the ideal formula is V_7S_8, which corresponds to V 58.16%, S 41.84%, total 100 wt.%. The density, based on the empirical formula and unit-cell volume refined form single-crystal structure XRD data, is 4.545 g·cm^{-3}. The mineral is trigonal, space group $P3_221$, with a = 6.689(3) Å, c = 17.403(6) Å, V = 674.4(5) Å^3, Z = 3, and exhibits a twelve-fold superstructure ($2a \times 2a \times 3c$) of the NiAs-type subcell with V-atoms octahedrally coordinated by S atoms. The distribution of vacancies is discussed in relation to other pyrrhotite-like compounds. The mineral name is for Dr. Demetrios Eliopoulos (1947–2019), a geoscientist at the Institute of Geology and Mineral Exploration (IGME) of Greece and his widow, Prof. Maria Eliopoulos (nee Economou, 1947), University of Athens, Greece, for their contributions to the knowledge of ore deposits of Greece and to the mineralogical, petrographic, and geochemical studies of ophiolites, including the Othrys complex. The mineral and its name have been approved by the Commission of New Minerals, Nomenclature, and Classification of the International Mineralogical Association (No. 2019-96).

Keywords: eliopoulosite; sulfide; chromitite; Agios Stefanos mine; Othrys; ophiolite; Greece

1. Introduction

Only eight minerals containing V and S are in the list of valid species approved by the International Mineralogical Association (IMA). They include, in alphabetic order: colimaite, K_3VS_4 [1]; colusite,

$Cu_{13}VAs_3S_{16}$ [2]; germanocolusite, $Cu_{13}VGe_3S_{16}$ [3]; merelaniite, $Mo_4Pb_4VSbS_{15}$ [4]; nekrasovite, $Cu_{13}VSn_3S_{16}$ [5]; patronite, VS_4 [6]; stibiocolusite, $Cu_{13}V(Sb,Sn,As)_3S_{16}$ [7]; and sulvanite, Cu_3VS_4 [8]. All of them, with the exception of patronite, a mineral discovered in 1906 in the Minas Ragra of Peru [6], are sulfides or sulfosalts characterized by a complex composition including other metals besides vanadium.

During a recent investigation of the heavy mineral concentrates from a chromitite collected in the Othrys ophiolite (central Greece), three new minerals were discovered. Two of them are phosphides, namely tsikourasite, $Mo_3Ni_2P_{1+x}$ [9] and grammatikopoulosite, NiVP [10]. A chemical and structural study revealed the third mineral to be a new sulfide, trigonal in symmetry and having the ideal formula V_7S_8. The mineral and its name were approved by the Commission of New Minerals, Nomenclature and Classification of the International Mineralogical Association (No. 2019-096). The new mineral has been named after Dr. Demetrios Eliopoulos (1947–2019), a geoscientist at the Institute of Geology and Mineral Exploration (IGME) of Greece and his widow, Prof. Maria Eliopoulos (nee Economou, 1947), University of Athens, Greece, for their contributions to the knowledge of ore deposits of Greece and to the mineralogical, petrographic, and geochemical studies of ophiolites, including the Othrys complex. Holotype material is deposited in the Mineralogical Collection of the Museo di Storia Naturale, Università di Pisa, Via Roma 79, Calci (Pisa, Italy), under catalogue number 19911 (same type specimen of grammatikopoulosite).

2. Geological Background and Occurrence of Eliopoulosite

Eliopoulosite was discovered in a heavy-mineral concentrate obtained from massive chromitite collected in the mantle sequence of the Mesozoic Othrys ophiolite, located in central Greece (Figure 1A). The geology, petrography, and geodynamic setting of the Otrhys ophiolite have been discussed by several authors [11–24]. The studied sample was collected in the abandoned chromium mine of Agios Stefanos, located a few km southwest of the Domokos village (Figure 1B). In the studied area, a mantle tectonite composed of plagioclase lherzolite, harzburgite, and minor harzburgite-dunite occurs in contact with rocks of the crustal sequence (Figure 1C). The investigated chromitite was collected from the harzburgite-dunite that is cut across by several dykes of gabbro (Figure 1C).

The ophiolite of Othrys is a complete but dismembered suite (Mirna Group) and consists of three structural units: the uppermost succession with variably serpentinized peridotites, which is structurally bounded by an ophiolite mélange; the intermediate Kournovon dolerite, including cumulate gabbro and local rhyolite; and the lower Sipetorrema Pillow Lava unit also including basaltic flows, siltstones, and chert. The Mirna Group constitutes multiple inverted thrust sheets, which were eventually obducted onto the Pelagonian Zone, during the Late Jurassic-Early Cretaceous [11–14]. Three types of basalts with different geochemical signatures have been described: i) alkaline within-plate (WPB), occurring in the mélange, which is related to oceanic seamounts or to ocean-continent transition zones; ii) normal-type mid-ocean ridge (N-MORB); and iii) low-K tholeiitic (L-KT) rocks, which are erupted close to the rifted margin of an ocean-continent transition zone. Radiolarian data from interbedded cherts suggest Middle to Late Triassic ages [15]. The Othrys ophiolite is structurally divided into the west and east Othrys suites, which are thought to derive from different geotectonic environments. The former is related to an extension regime (back-arc basin or MORB [16–18]), while the latter formed in a supra-subduction zone (SSZ) setting [17–19]. This difference is reflected in the contrasting geochemical compositions of their ultramafic rocks, as well as in the diverse platinum group minerals (PGM) assemblages of their host chromitites [20,21], which suggest large mantle heterogeneities in this area. Conflicting views with regards to the evolution of the Othrys ophiolite suggest the involvement of Pindos [11,22,23] or Vardar (Axios) [15] oceanic domains.

The studied spinel-supergroup minerals that host eliopoulosite can been classified as magnesiochromite, although their composition is rather heterogeneous [9,10,25] with the amounts of Cr_2O_3 (44.96–51.64 wt.%), Al_2O_3 (14.18–20.78 wt.%), MgO (13.34–16.84 wt.%), and FeO (8.3–13.31 wt.%) varying significantly through the sampled rock. The calculated Fe_2O_3 is relatively high, and ranges

from 6.72 to 9.26 wt.%. The amounts of MnO (0.33–0.60 wt.%), V_2O_3 (0.04–0.30 wt.%), ZnO (up to 0.07 wt.%), and NiO (0.03–0.24 wt.%) are low. The maximum TiO_2 content is 0.23 wt.%, which is typical for the podiform chromitites hosted in the mantle sequence of ophiolite complexes.

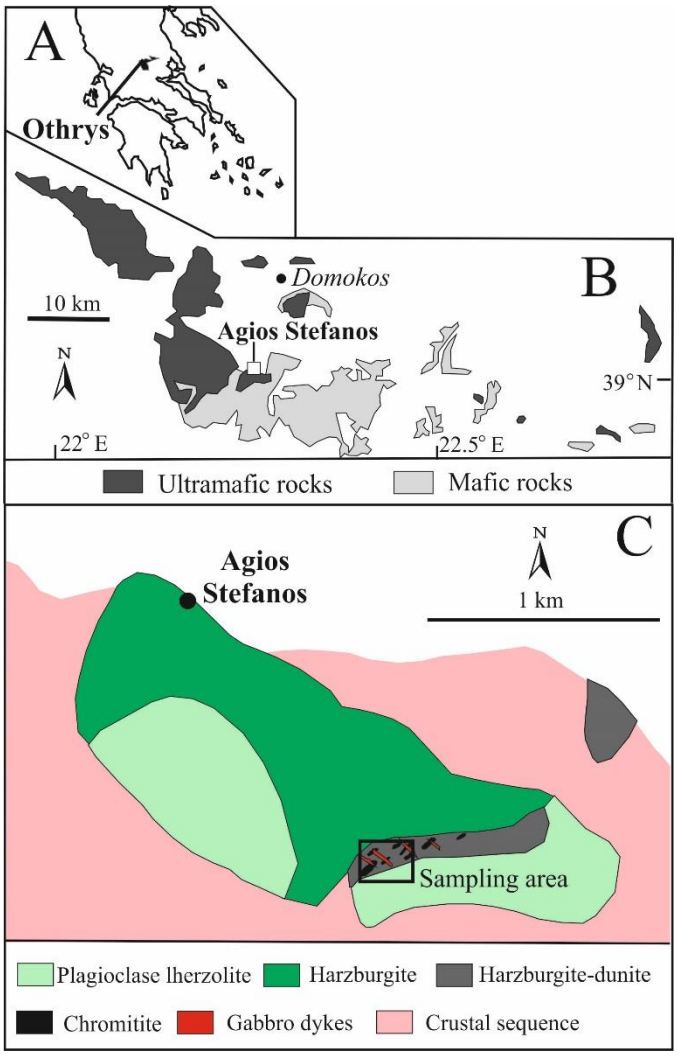

Figure 1. Location of the Othrys complex in Greece (**A**); general geological map of the Othrys ophiolite showing the location of the Agios Stefanos chromium mine (**B**) and (**C**) detailed geological setting of the Agios Stefanos area (modified after [10] and [5]).

3. Analytical Methods

The heavy minerals were concentrated at SGS Mineral Services, Canada, following the methodology described by several authors [9,10,21,25,26]. After the concentration process, the heavy minerals were embedded in epoxy blocks and then polished for mineralogical examination.

Quantitative chemical analyses and acquisition of back-scattered electron images of eliopoulosite were performed with a JEOL JXA-8200 electron-microprobe, installed in the E. F. Stumpfl laboratory, Leoben University, Austria, operating in wavelength dispersive spectrometry (WDS) mode. Major and minor elements were determined at 20 kV accelerating voltage and 10 nA beam current, with 20 s as the counting time for the peak and 10 s for the backgrounds. The beam diameter was about 1 μm in size. For the WDS analyses, the following lines and diffracting crystals were used: S = ($K\alpha$, PETJ), V, Ni, Fe, Co = ($K\alpha$, LIFH), and Mo = ($L\alpha$, PETJ). The following standards were selected: metallic vanadium for V, pyrite for S and Fe, millerite for Ni, molybdenite for Mo, and skutterudite for Co.

The ZAF correction method was applied. Automatic correction was performed for interference Mo-S. Representative analyses of eliopoulosite are listed in Table 1.

Table 1. Electron microprobe analyses (wt.%) of eliopoulosite.

Analysis	S	V	Ni	Fe	Co	Mo	Total
1	41.34	53.08	1.24	0.87	0.48	0.55	99.01
2	41.35	53.45	1.33	0.92	0.52	0.57	99.29
3	41.36	53.55	1.39	0.97	0.55	0.57	99.37
4	41.39	53.71	1.41	1.00	0.55	0.57	99.43
5	41.42	53.90	1.51	1.01	0.61	0.58	99.72
6	41.44	53.91	1.54	1.09	0.63	0.59	99.75
7	41.57	53.97	1.55	1.09	0.63	0.59	99.77
8	41.65	54.03	1.58	1.09	0.63	0.60	99.82
9	41.67	54.03	1.65	1.10	0.64	0.63	99.86
10	41.73	54.06	1.67	1.11	0.64	0.64	99.92
11	41.76	54.09	1.69	1.11	0.65	0.65	100.18
12	41.82	54.16	1.70	1.12	0.68	0.67	100.20
13	41.90	54.21	1.72	1.12	0.69	0.68	100.26
14	41.94	54.25	1.72	1.13	0.72	0.68	100.27
15	41.99	54.40	1.94	1.16	0.72	0.69	100.28
16	42.03	54.40	1.99	1.16	0.73	0.69	100.31
17	42.12	54.56	2.02	1.18	0.76	0.70	100.78
18	42.28	54.64	2.13	1.19	0.78	0.75	100.78
19	42.33	54.80	2.22	1.21	0.79	0.81	100.84
20	42.62	55.02	2.27	1.47	0.91	0.90	100.84
average	41.78	54.11	1.71	1.1	0.67	0.66	100.03

A small grain of eliopoulosite was hand-picked from the polished section under a reflected light microscope. The crystal (about 80 μm in size) was carefully and repeatedly washed in acetone and mounted on a 5 μm-diameter carbon fiber, which was, in turn, attached to a glass rod in preparation of the single-crystal X-ray diffraction measurements.

Single-crystal X-ray diffraction data were collected at the University of Florence (Italy) using a Bruker D8 Venture equipped with a Photon II CCD detector, with graphite-monochromatized Mo$K\alpha$ radiation ($\lambda = 0.71073$ Å). Intensity data were integrated and corrected for standard Lorentz-polarization factors with the software package *Apex*3 [27,28]. A total of 1289 unique reflections was collected up to $2\theta = 62.24°$.

The reflectance measurements on eliopoulosite were carried out using a WTiC standard and a J&M TIDAS diode array spectrophotometer at the Natural History Museum of London, UK.

4. Physical and Optical Properties

In the polished section, eliopoulosite occurs as tiny crystals (from 5 μm up to about 80 μm) and is anhedral to subhedral in habit. It consists of polyphase grains associated with other minerals, such as tsikourasite, nickelphosphide, awaruite, and grammatikopoulosite (Figure 2).

In plane-reflected polarized light, eliopoulosite is grayish-brown and shows no internal reflections, bireflectance, and pleochroism. It is weakly anisotropic, with colors varying from light to dark greenish. Reflectance values of the mineral in air (R in %) are listed in Table 2 and shown in Figure 3.

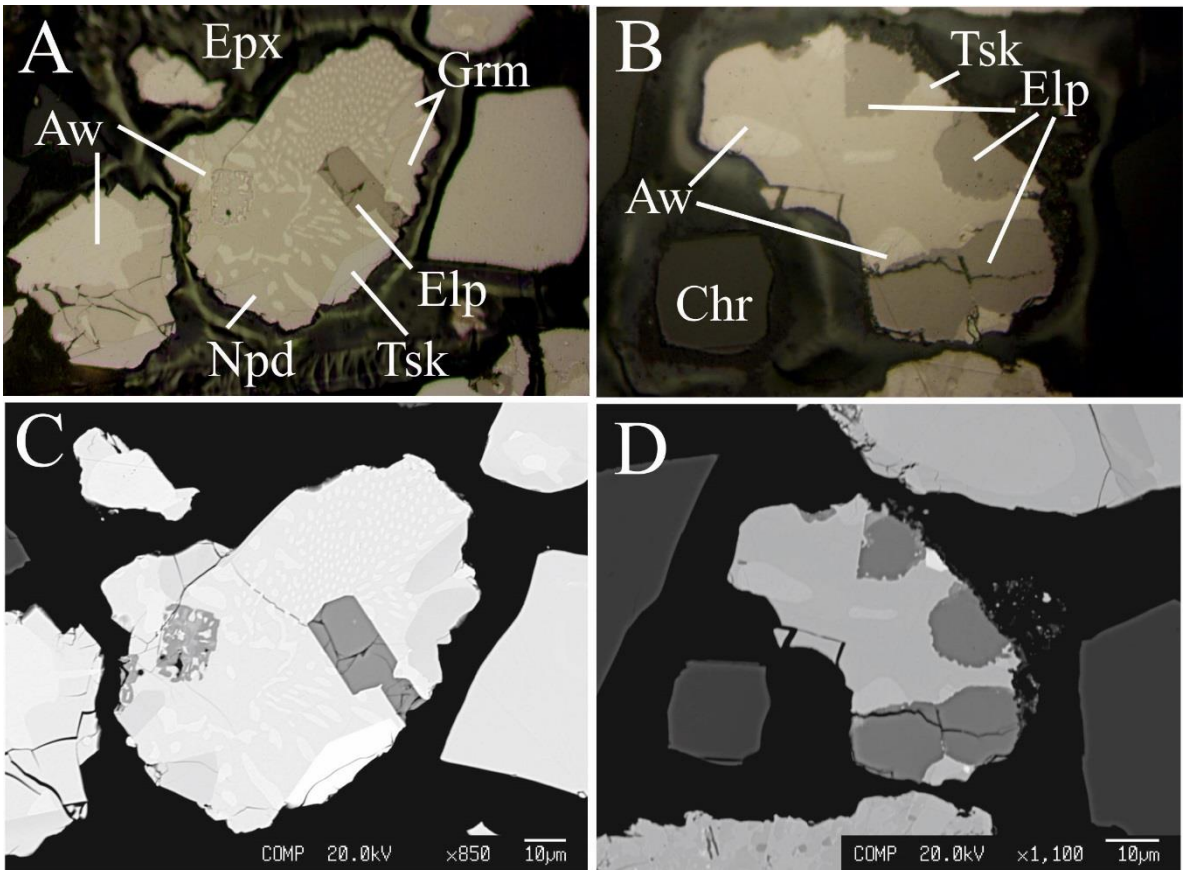

Figure 2. Digital image in reflected plane polarized light (**A**,**B**) and back-scattered electron image (**C**,**D**) showing eliopoulosite from the chromitite of Agios Stefanos. Abbreviations: Elp = eliopoulosite, Grm = grammatikopoulosite, Tsk = tsikourasite, Aw = awaruite, Npd = nickelphosphide, Chr = chromite, Epx = epoxy.

Table 2. Reflectance values of eliopoulosite, those required by the Commission on Ore Mineralogy (COM) are given in bold.

λ (nm)	R_o (%)	$R_{e'}$ (%)
400	32.0	33.1
420	32.7	33.7
440	33.5	34.5
460	34.3	35.3
470	**34.8**	**35.7**
480	35.2	36.1
500	36.1	37.0
520	36.9	37.8
540	37.7	38.7
546	**38.0**	**39.0**
560	38.6	39.7
580	39.5	40.8
589	**40.0**	**41.3**
600	40.5	41.9
620	41.2	42.9
640	42.1	43.8
650	**42.5**	**44.2**
660	42.8	44.6
680	43.5	45.5
700	44.3	46.2

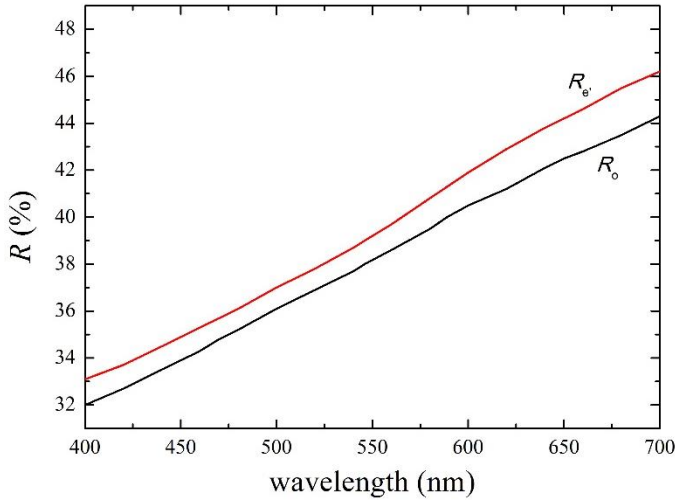

Figure 3. Reflectance data for eliopoulosite.

Due to the small amount of available material, density was not measured. The calculated density was = 4.545 g·cm^{-3}, based on the empirical formula and the unit-cell volume refined from single-crystal XRD data.

5. X-Ray Crystallography and Chemical Composition

The mineral is trigonal, with a = 6.689(3) Å, c = 17.403(6) Å, V = 674.4(5) Å^3, and Z = 3. The reflection conditions (*00l*: $l = 3n$), together with the observed R_{int} in the different Laue classes, point unequivocally to the choice of the space group $P3_221$. The structure solution was then carried out in this space group. The positions of most of the atoms (all the V positions and most of the S atoms) were determined by means of direct methods [29]. A least-squares refinement on F^2 using these heavy-atom positions and isotropic temperature factors produced an R factor of 0.123. Three-dimensional difference Fourier synthesis yielded the position of the remaining sulfur atoms. The program Shelxl-97 [30] was used for the refinement of the structure. The site occupancy factor (s.o.f.) at the cation sites was allowed to vary (V vs. structural vacancy) using scattering curves for neutral atoms taken from the International Tables for Crystallography [30]. Four V sites (i.e., V1, V2, V3, and V4) were found to be partially occupied by vanadium (75%), while V5 and V6 were found to be fully occupied by V and fixed accordingly. Sulfur atoms were found on four fully occupied general positions leading to an ideal formula V_7S_8. Given the almost identical partial occupancy of four V sites (i.e., 75%), we carefully checked either the possible presence of twinning or the acentricity of the model. The lack of the inversion center was confirmed using the Flack parameter in Shelxl (0.07(1)) and the trigonal model was double-checked with the Platon *addsymm* routine. At the last stage, with anisotropic atomic displacement parameters for all atoms and no constraints, the residual value settled at $R1$ = 0.0363 for 398 observed reflections ($Fo > 4\sigma(Fo)$) and 79 parameters and at $R1$ = 0.0537 for all 1289 independent reflections. Refined atomic coordinates and isotropic displacement parameters are given in Table 3, whereas selected bond distances are reported in Table 4. Crystallographic Information File (CIF) is deposited.

The calculated X-ray powder diffraction pattern (Table 5) was computed on the basis of the unit-cell data above and with the atom coordinates and occupancies reported in Table 3.

Table 3. Atoms, site occupancy, fractional atom coordinates (Å), and isotropic atomic displacement parameters (Å^2) for eliopoulosite.

Atom	Site Occupancy	*x/a*	*y/b*	*z/c*	U_{iso}
V1	$V_{0.749(6)}$	0.0001(6)	0	2/3	0.0088(6)
V2	$V_{0.762(6)}$	0.5005(6)	0	2/3	0.0095(6)
V3	$V_{0.755(6)}$	0.0006(7)	0	1/6	0.0113(6)
V4	$V_{0.749(7)}$	0.5010(7)	0	1/6	0.0187(8)
V5	$V_{1.00}$	0.4996(4)	0.4997(5)	0.16664(5)	0.0060(3)
V6	$V_{1.00}$	0.4997(5)	0.4996(5)	0.33327(5)	0.0120(4)
S1	$S_{1.00}$	0.1663(7)	0.3343(6)	0.08309(11)	0.0227(4)
S2	$S_{1.00}$	0.1659(7)	0.3328(7)	0.41639(11)	0.0226(4)
S3	$S_{1.00}$	0.1661(7)	0.3331(6)	0.74976(11)	0.0226(4)
S4	$S_{1.00}$	0.3333(6)	0.6673(7)	0.25009(11)	0.0228(4)

Table 4. Bond distances (Å) in the structure of eliopoulosite.

V1-S2	2.409(5) (×2)	V5-S1	2.413(4)
V1-S3	2.411(3) (×2)	V5-S4	2.416(3)
V1-S1	2.418(4) (×2)	V5-S1	2.417(4)
mean	2.413	V5-S2	2.418(4)
		V5-S4	2.419(3)
V2-S1	2.412(4) (×2)	V5-S3	2.419(4)
V2-S2	2.413(5) (×2)	mean	2.417
V2-S4	2.414(3) (×2)		
mean	2.413	V6-S1	2.407(4)
		V6-S4	2.411(4)
V3-S3	2.414(4) (×2)	V6-S3	2.413(4)
V3-S2	2.418(3) (×2)	V6-S3	2.413(4)
V3-S1	2.422(3) (×2)	V6-S2	2.415(4)
mean	2.418	V6-S4	2.417(4)
		mean	2.413
V4-S4	2.413(3) (×2)		
V4-S2	2.417(4) (×2)		
V4-S3	2.421(5) (×2)		
mean	2.417		
V1-V3	2.9006(10) (×2)		
V2-V5	2.9001(13) (×2)		
V4-V6	2.9018(14) (×2)		
V5-V6	2.8998(12) (×2)		

Table 5. Calculated X-ray powder diffraction data (d in Å) for eliopoulosite. The strongest observed reflections are given in bold.

hkl	d_{calc}	I_{calc}
200	**2.8964**	**29**
023	**2.5914**	**45**
026	**2.0495**	**100**
220	**1.6723**	**40**
029	1.6082	10
012	1.4503	8
400	1.4482	3
046	1.2957	20
22$\underline{12}$	1.0956	15
246	1.0242	12
600	0.9655	4

The chemical data (Table 1), yielding to a mean composition (wt.%) of S 41.78, V 54.11, Ni 1.71, Fe 1.1, Co 0.67, Mo 0.66, and total 100.03, were then normalized taking into account the structural results. The empirical formula of eliopoulosite on the basis of Σatoms = 15 apfu is $(V_{6.55}Ni_{0.19}Fe_{0.12}Co_{0.07}Mo_{0.04})_{\Sigma = 6.97}S_{8.03}$. The simplified formula is $(V,Ni,Fe)_7S_8$ and the ideal formula is V_7S_8, which corresponds to V 58.16, S 41.84, and total 100 (wt.%).

The structure can be considered as a twelve-fold superstructure ($2a \times 2a \times 3c$) of the NiAs-type subcell with V atoms octahedrally coordinated by S atoms and sulfur located in a trigonal prism. There are six octahedral layers in the structure with rods of fully occupied V sites alternate to rods of partially occupied sites, so that every layer contains 3.5 vanadium atoms. In successive layers rods are directed along [110], [100], and [010] accordingly to the threefold screw axis. As shown in Figure 5, the distribution of fully (blue in color) and partially (pale blue) occupied sites determine the superstructure along the $\mathbf{a_1}$ and $\mathbf{a_2}$ axes. Differences in electron density between fully and partially occupied sites are indeed rather modest (22 vs. 16.5): Accordingly, *hkl* reflections with $h,k = 2n + 1$ are rather weak ($\langle I/\sigma(I)\rangle$ = 27.1 vs. 4890.3).

Since the octahedral vacancies' distribution within the layers at $z = 0$, $z = 1/6$, and $z = 1/3$ is perfectly replicated at layers at $z = 1/2$, $z = 2/3$, and $z = 5/6$ (Figure 5), no contribution to *hkl* reflections with $l = 2n + 1$ is given by metal atoms. However, their intensities ($\langle I/\sigma(I)\rangle$ = 564.3 vs. 3349.2) are even higher than those leading to doubling of **a**-axis, due to the different position of sulfur atoms related to the different octahedral orientation in the layer at $z = 0$ with respect to $z = 1/2$ (Figure 4).

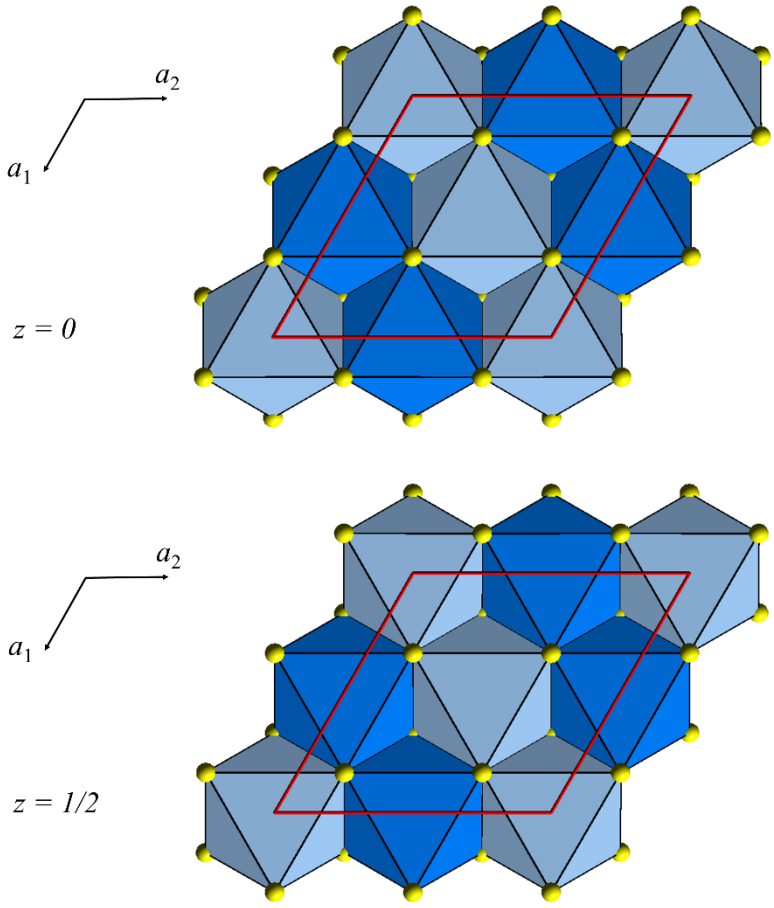

Figure 4. Octahedral layers in eliopoulosite projected down [001]. Layer at $z = 0$ (top of picture) repeats at $z = 1/3$ and $z = 2/3$; layer at $z = 1/2$ (bottom of picture) repeats at $z = 1/6$ and $z = 5/6$. Blue and pale blue colors represent full and partial occupancy. Sulfur atoms are depicted in yellow. The unit cell and the orientation of the structure are indicated.

The eliopoulosite structure shows strong analogies with the superstructures observed in the pyrrhotite-group of minerals. It is identical to the structure inferred for synthetic $VS_{1.125}$ [31]. The mean <V-S> bond distances in eliopoulosite (in the range 2.413–2.418 Å) are in excellent agreement with those found for synthetic vanadium sulfides. To achieve the charge balance, one should hypothesize the presence of both divalent and trivalent vanadium in eliopoulosite (i.e., $V^{2+}{}_5V^{3+}{}_2S_8$). The octahedral sites, however, do not show any significant difference symptomatic of a V^{2+}-V^{3+} ordering. Likewise, we did not find any evidence of ordering of the minor substituents (i.e., Ni and Fe) at a particular structural site. Furthermore, eliopoulosite shows, for the analogy of stoichiometry, unit cell and space group, close relationships with the metastable, trigonal form of 3C-Fe_7S_8 (a = 6.852(6), c = 17.046(2), $P3_121$) [32]. However, the distribution of vacancies is quite different (Figure 5b): As in other types of pyrrhotites [33], in 3C-Fe_7S_8 octahedral vacancies are completely ordered on one position alone so that the layers containing a void (i.e., three metal atoms) are alternating with fully occupied layers (i.e., four metal atoms).

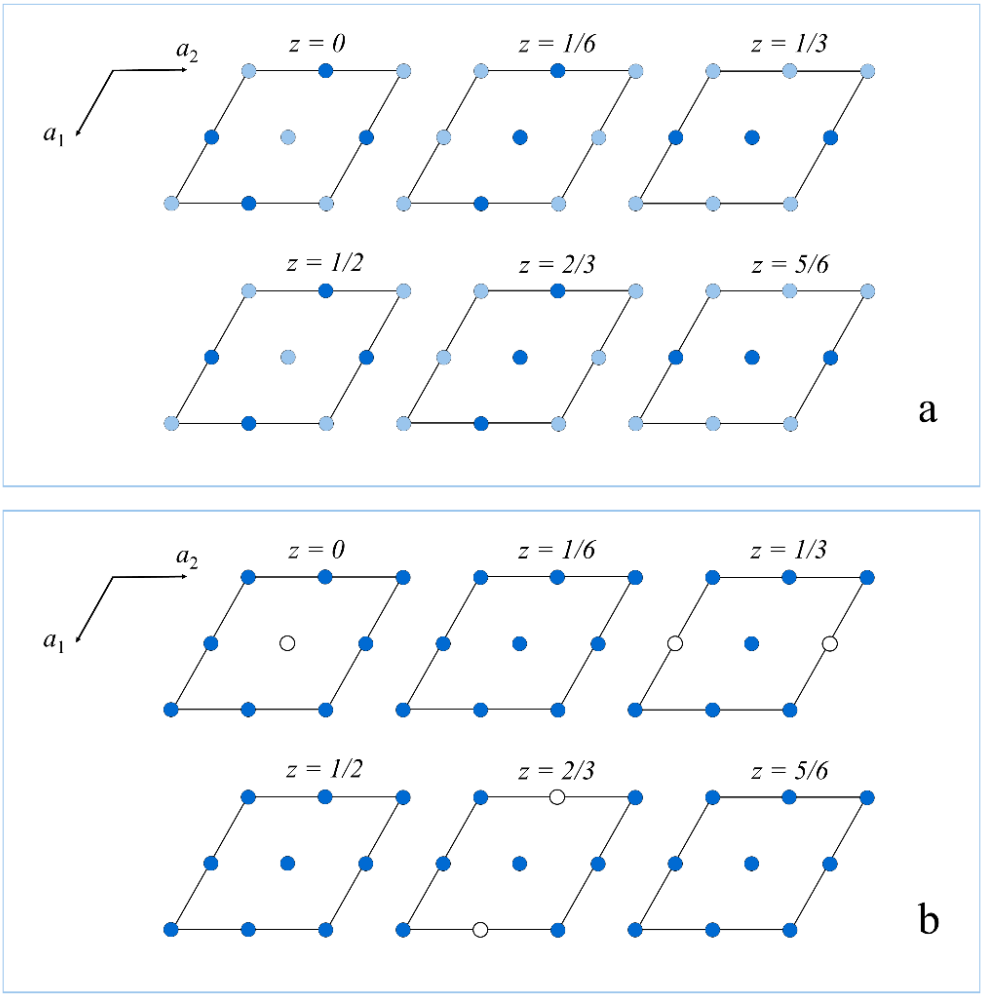

Figure 5. Metal distribution in eliopoulosite (**a**) and in synthetic 3C-Fe_7S_8 pyrrhotite (**b**). Blue and pale blue circles refer to metal positions with full and partial (75%) occupancy, respectively. White circles represent completely empty sites in synthetic 3C-Fe_7S_8 pyrrhotite [32]. The unit cell and the orientation of the structure are indicated.

Eliopoulosite does not correspond to any valid or invalid unnamed mineral [34]. According to literature data [1–8] eliopoulosite is the ninth mineral containing V and S that has been accepted by IMA. Noteworthy, eliopoulosite is the second V^{2+}-bearing mineral, the first being dellagiustaite, Al_2VO_4 [35]. The presence of divalent V requires extremely reducing conditions (well below the iron-wüstite buffer). Furthermore, based on its chemical composition, eliopoulosite is the second sulfide that contains only V as a major component discovered so far. Recently, Ivanova et al. [36] reported on the presence of a V,Cr,Fe-sulfide in the extremely reduced assemblage of a rare CB chondrite. Due to its small size (one micron) the grain was studied only by EBSD (Electron BackScattered Diffraction) and no crystallographic or optical data were provided. However, its ideal composition $(V,Cr,Fe)_4S_5$ seems different compared to that of eliopoulosite in terms of S content and V/Fe ratio and the presence of abundant Cr.

Interestingly, Selezneva et al. [37] recently showed that synthetic V_7S_8 shows differences in the magnetic behavior with respect to trigonal Fe_7S_8. Indeed, V_7S_8 is observed to exhibit a Pauli-paramagnetic behavior opposite to the classic ferrimagnetic ordering usually observed in pyrrhotite. Unfortunately, the small amount of the natural material precludes any possible measurement of both the magnetic susceptibility and magnetization. Such an experiment would have allowed us to verify if the amount of structural vacancies observed for eliopoulosite are enough to compensate the magnetic moments to avoid the ferromagnetic order.

6. Remarks on the Origin of Eliopoulosite

Eliopoulosite was found in the same sample in which tsikourasite and grammatikopoulosite were discovered, and the three minerals occur in the same mineralogical assemblage [9,10]. Therefore, we can argue that they formed under the same chemical-physical condition (i.e., in a strongly reducing environment). This assumption is fully supported by the chemical composition of eliopoulosite, that points to a low valence state for V. However, as already proposed for the origin of tsikourasite and grammatikopoulosite, it is still not possible to provide a conclusive model to explain exhaustively the genesis of eliopoulosite. The following hypothesis can be formulated, since all of them imply the presence of a reducing environment [9,10,38–43]: i) low-temperature alteration of chromitite during serpentinization process; ii) high-temperature reaction of the chromitites with reducing fluids, at mantle depth; iii) post-orogenic surface lightning strike; or iv) meteorite impact.

However, the probability of intercepting a fragment of a meteorite or a fulgurite in the Otrhys ophiolite during the sampling of the studied chromitite seems very unlikely, although a V-bearing sulfide has been reported in a meteorite [36].

Supplementary Materials: The following are available online at http://www.mdpi.com/2075-163X/10/3/245/s1, CIF: eliopoulosite.

Author Contributions: L.B., F.Z., and P.B. wrote the manuscript; F.Z. performed the chemical analyses; L.B. and P.B. performed the diffraction experiments; T.G. and B.T. provided the concentrate sample and information on the sample provenance and petrography of Othrys chromitite; G.G. discussed the chemical data and C.S. obtained the optical data. All the authors provided support in the data interpretation and revised the manuscript. All authors have read and agreed to the published version of the manuscript.

Funding: The authors are grateful to the University Centrum for Applied Geosciences (UCAG) for the access to the E. F. Stumpfl electron microprobe laboratory. SGS Mineral Services, Canada, is thanked to have performed the concentrate sample. S. Karipi is thanked for sample collection and participating in the field work. L.B. thanks MIUR, project "TEOREM deciphering geological processes using Terrestrial and Extraterrestrial ORE Minerals", prot. 2017AK8C32 (PI: Luca Bindi).

Acknowledgments: The authors acknowledge Ritsuro Miyawaki, Chairman of the CNMNC and its members for helpful comments on the submitted new mineral proposal. Many thanks are due to the editorial staff of Minerals.

Conflicts of Interest: The authors declare no conflicts of interest.

References

1. Ostrooumov, M.; Taran, Y.; Arellano-Jimenez, M.; Ponse, A.; Reyes-Gasga, J. Colimaite, K_3VS_4—A new potassium-vanadium sulfide mineral from the Colima volcano, State of Colima (Mexico). *Rev. Mex. Cienc. Geol.* **2009**, *26*, 600–608.
2. Zachariasen, W.H. X-Ray examination of colusite, $(Cu,Fe,Mo,Sn)_4(S,As,Te)_{3–4}$. *Am. Mineral.* **1933**, *18*, 534–537.
3. Spiridonov, E.M.; Kachalovskaya, V.M.; Kovachev, V.V.; Krapiva, L.Y. Germanocolusite $Cu_{26}V_2(Ge,As)_6S_{32}$—a new mineral. *Vest. Moskov. Univers., Ser. 4, Geologiya* **1992**, *1992*, 50–54. (In Russian)
4. Jaszczak, J.A.; Rumsey, M.S.; Bindi, L.; Hackney, S.A.; Wise, M.A.; Stanley, C.J.; Spratt, J. Merelaniite, $Mo_4Pb_4VSbS_{15}$, a new molybdenum-essential member of the cylindrite group, from the Merelani Tanzanite Deposit, Lelatema Mountains, Manyara Region, Tanzania. *Minerals* **2016**, *6*, 115. [CrossRef]
5. Kovalenker, V.A.; Evstigneeva, T.L.; Malov, V.S.; Trubkin, N.V.; Gorshkov, A.I.; Geinke, V.R. Nekrasovite $Cu_{26}V_2Sn_6S_{32}$—A new mineral of the colusite group. *Mineral. Zh.* **1984**, *6*, 88–97.
6. Hillibrand, W.F. Vanadium sulphide, patronite, and its mineral associates from Minasragra, Peru. *Am. J. Sci.* **1907**, *24*, 141–151. [CrossRef]
7. Spiridonov, E.M.; Badalov, A.S.; Kovachev, V.V. Stibiocolusite $Cu_{26}V_2(Sb,Sn,As)_6S_{32}$: A new mineral. *Dokl. Akad. Nauk* **1992**, *324*, 411–414. (In Russian)
8. Trojer, F.J. Refinement of the structure of sulvanite. *Am. Mineral.* **1996**, *51*, 890–894.
9. Zaccarini, F.; Bindi, L.; Ifandi, E.; Grammatikopoulos, T.; Stanley, C.; Garuti, G.; Mauro, D. Tsikourasite, $Mo_3Ni_2P_{1+x}$ ($x < 0.25$), a new phosphide from the chromitite of the Othrys Ophiolite, Greece. *Minerals* **2019**, *9*, 248.
10. Bindi, L.; Zaccarini, F.; Ifandi, E.; Tsikouras, B.; Stanley, C.; Garuti, G.; Mauro, D. Grammatikopoulosite, NiVP, a new phosphide from the chromitite of the Othrys Ophiolite, Greece. *Minerals* **2020**, *10*, 131. [CrossRef]
11. Smith, A.G.; Rassios, A. The evolution of ideas for the origin and emplacement of the western Hellenic ophiolites. *Geol. Soc. Am. Spec. Pap.* **2003**, *373*, 337–350.
12. Hynes, A.J.; Nisbet, E.G.; Smith, G.A.; Welland, M.J.P.; Rex, D.C. Spreading and emplacement ages of some ophiolites in the Othris region (Eastern Central Greece). *Z. Deutsch Geol. Ges.* **1972**, *123*, 455–468.
13. Smith, A.G.; Hynes, A.J.; Menzies, M.; Nisbet, E.G.; Price, I.; Welland, M.J.; Ferrière, J. The stratigraphy of the Othris Mountains, Eastern Central Greece: A deformed Mesozoic continental margin sequence. *Eclogue Geol. Helv.* **1975**, *68*, 463–481.
14. Rassios, A.; Smith, A.G. Constraints on the formation and emplacement age of western Greek ophiolites (Vourinos, Pindos, and Othris) inferred from deformation structures in peridotites. In *Ophiolites and Oceanic Crust: New Insights from Field Studies and the Ocean Drilling Program*; Dilek, Y., Moores, E., Eds.; Geological Society of America Special Paper: Boulder, CO, USA, 2001; pp. 473–484.
15. Bortolotti, V.; Chiari, M.; Marcucci, M.; Photiades, A.; Principi, G.; Saccani, E. New geochemical and age data on the ophiolites from the Othrys area (Greece): Implication for the Triassic evolution of the Vardar ocean. *Ofioliti* **2008**, *33*, 135–151.
16. Barth, M.G.; Mason, P.R.D.; Davies, G.R.; Drury, M.R. The Othris Ophiolite, Greece: A snapshot of subduction initiation at a mid-ocean ridge. *Lithos* **2008**, *100*, 234–254. [CrossRef]
17. Barth, M.; Gluhak, T. Geochemistry and tectonic setting of mafic rocks from the Othris Ophiolite, Greece. *Contr. Mineral. Petrol.* **2009**, *157*, 23–40. [CrossRef]
18. Dijkstra, A.H.; Barth, M.G.; Drury, M.R.; Mason, P.R.D.; Vissers, R.L.M. Diffuse porous melt flow and melt-rock reaction in the mantle lithosphere at a slow-spreading ridge: A structural petrology and LA-ICP-MS study of the Othris Peridotite Massif (Greece). *Geochem. Geophys. Geosyst.* **2003**, *4*, 278. [CrossRef]
19. Magganas, A.; Koutsovitis, P. Composition, melting and evolution of the upper mantle beneath the Jurassic Pindos ocean inferred by ophiolitic ultramafic rocks in East Othris, Greece. *Int. J. Earth Sci.* **2015**, *104*, 1185–1207. [CrossRef]
20. Garuti, G.; Zaccarini, F.; Economou-Eliopoulos, M. Paragenesis and composition of laurite from chromitites of Othrys (Greece): Implications for Os-Ru fractionation in ophiolite upper mantle of the Balkan Peninsula. *Mineral. Dep.* **1999**, *34*, 312–319. [CrossRef]

21. Tsikouras, B.; Ifandi, E.; Karipi, S.; Grammatikopoulos, T.A.; Hatzipanagiotou, K. Investigation of platinum-group minerals (PGM) from Othrys chromitites (Greece) using superpanning concentrates. *Minerals* **2016**, *6*, 94. [CrossRef]
22. Robertson, A.H.F. Overview of the genesis and emplacement of Mesozoic ophiolites in the Eastern Mediterranean Tethyan region. *Lithos* **2002**, *65*, 1–67. [CrossRef]
23. Robertson, A.H.F.; Clift, P.D.; Degnan, P.; Jones, G. Palaeogeographic and palaeotectonic evolution of the Eastern Mediterranean Neotethys. *Palaeogeogr. Palaeoclim. Palaeoecol.* **1991**, *87*, 289–343. [CrossRef]
24. Economou, M.; Dimou, E.; Economou, G.; Migiros, G.; Vacondios, I.; Grivas, E.; Rassios, A.; Dabitzias, S. Chromite deposits of Greece. In *Chromites, UNESCO's IGCP197 Project Metallogeny of Ophiolites*; Petrascheck, W., Karamata, S., Eds.; Theophrastus Publ. S.A.: Athens, Greece, 1986; pp. 129–159.
25. Ifandi, E.; Zaccarini, F.; Tsikouras, B.; Grammatikopoulos, T.; Garuti, G.; Karipi, S.; Hatzipanagiotou, K. First occurrences of Ni-V-Co phosphides in chromitite of Agios Stefanos mine, Othrys ophiolite, Greece. *Ofioliti* **2018**, *43*, 131–145.
26. Zaccarini, F.; Ifandi, E.; Tsikouras, B.; Grammatikopoulos, T.; Garuti, G.; Mauro, D.; Bindi, L.; Stanley, C. Occurrences of new phosphides and sulfide of Ni, Co, V, and Mo from chromitite of the Othrys ophiolite complex (Central Greece). *Per. Mineral.* **2019**, 88. [CrossRef]
27. Bruker. *APEX3*; Bruker AXS Inc.: Madison, WI, USA, 2016. Available online: https://www.bruker.com/products/x-ray-diffraction-and-elemental-analysis/single-crystal-x-ray-diffraction/sc-xrd-software/apex3.html (accessed on 6 March 2020).
28. Bruker. *SAINT and SADABS*; Bruker AXS Inc.: Madison, WI, USA, 2016. Available online: https://www.bruker.com/products/x-ray-diffraction-and-elemental-analysis/single-crystal-x-ray-diffraction/sc-xrd-software/apex3.html (accessed on 6 March 2020).
29. Sheldrick, G.M. A short history of SHELX. *Acta Crystallogr.* **2008**, *A64*, 112–122. [CrossRef]
30. Wilson, A.J.C. *International Tables for Crystallography: Mathematical, Physical, and Chemical Tables*; International Union of Crystallography: Chester, UK, 1992; Volume 3.
31. Grønvold, F.; Haraldsen, H.; Pedersen, B.; Tufte, T. X-ray and magnetic study of vanadium sulfides in the range V_5S_4 to V_5S_8. *Rev. Chim. Minéral.* **1969**, *6*, 215.
32. Nakano, A.; Tokonami, M.; Morimoto, N. Refinement of 3C pyrrhotite, Fe_7S_8. *Acta Crystallogr.* **1979**, *B35*, 722–724. [CrossRef]
33. Morimoto, N. Crystal structure of a monoclinic pyrrhotite. *Rec. Progr. Nat. Sci. Japan* **1978**, *3*, 183–206.
34. Smith, D.G.W.; Nickel, E.H. A system for codification for unnamed minerals: report of the Subcommittee for Unnamed Minerals of the IMA Commission on New Minerals, Nomenclature and Classification. *Can. Mineral.* **2007**, *45*, 983–1055. [CrossRef]
35. Cámara, F.; Bindi, L.; Pagano, A.; Pagano, R.; Gain, S.E.M.; Griffin, W.L. Dellagiustaite: A novel natural spinel containing V^{2+}. *Minerals* **2019**, *9*, 4. [CrossRef]
36. Ivanova, M.A.; Ma, C.; Lorenz, C.A.; Franchi, I.A.; Kononkova, N.N. A new unusual bencubbinite (cba), Sierra Gorda 013 with unique V-rich sulfides. *Met. Plan. Sci.* **2019**, *54*, 6149.
37. Selezneva, N.V.; Ibrahim, P.N.G.; Toporova, N.M.; Sherokalova, E.M.; Baranov, N.V. Crystal structure and magnetic properties of pyrrhotite-type compounds $Fe_{7-y}V_yS_8$. *Acta Phys. Polon.* **2018**, *A133*, 450–452. [CrossRef]
38. Malvoisin, B.; Chopin, C.; Brunet, F.; Matthieu, E.; Galvez, M.E. Low-temperature wollastonite formed by carbonate reduction: a marker of serpentinite redox conditions. *J. Petrol.* **2012**, *53*, 159–176. [CrossRef]
39. Etiope, G.; Tsikouras, B.; Kordella, S.; Ifandi, E.; Christodoulou, D.; Papatheodorou, G. Methane flux and origin in the Othrys ophiolite hyperalkaline springs, Greece. *Chem. Geol.* **2013**, *347*, 161–174. [CrossRef]
40. Etiope, G.; Ifandi, E.; Nazzari, M.; Procesi, M.; Tsikouras, B.; Ventura, G.; Steele, A.; Tardini, R.; Szatmari, P. Widespread abiotic methane in chromitites. *Sci. Rep.* **2018**, *8*, 8728. [CrossRef]
41. Xiong, Q.; Griffin, W.L.; Huang, J.X.; Gain, S.E.M.; Toledo, V.; Pearson, N.J.; O'Reilly, S.Y. Super-reduced mineral assemblages in "ophiolitic" chromitites and peridotites: The view from Mount Carmel. *Eur. J. Mineral.* **2017**, *29*, 557–570. [CrossRef]

42. Pasek, M.A.; Hammeijer, J.P.; Buick, R.; Gull, M.; Atlas, Z. Evidence for reactive reduced phosphorus species in the early Archean ocean. *Proc. Nat. Acad. Sci. U.S.A.* **2013**, *110*, 100089–100094. [CrossRef]
43. Ballhaus, C.; Wirth, R.; Fonseca, R.O.C.; Blanchard, H.; Pröll, W.; Bragagni, A.; Nagel, T.; Schreiber, A.; Dittrich, S.; Thome, V.; et al. Ultra-high pressure and ultra-reduced minerals in ophiolites may form by lightning strikes. *Geochem. Perspec. Lett.* **2017**, *5*, 42–46. [CrossRef]